SCIENTIFIC REPORTS

OPEN

Insight into the characteristics, removal, and toxicity of effluent organic matter from a pharmaceutical wastewater treatment plant during catalytic ozonation

Received: 8 March 2018
Accepted: 4 June 2018
Published online: 25 June 2018

Shuhan Wen, Lin Chen, Weiqi Li, Hongqiang Ren, Kan Li, Bing Wu, Haidong Hu & Ke Xu

Changes in the characteristics, removal efficiency, and toxicity of pharmaceutical effluent organic matter (EfOM) after catalytic ozonation were investigated in this study. After a 90-min treatment with a catalytic ozonation process (COP) in the presence of MnO_2 ceramsite, the total organic carbon (TOC), UV_{254}, colority, protein, and humic acid removal rates were 13.24%, 60.83%, 85.42%, 29.36% and 74.19%, respectively. The polysaccharide content increased by 12.73 mg/L during the COP for reaction times between 0 and ~50 min and decreased by 6.97 mg/L between 50 and ~90 min. Furthermore, 64.44% of the total colority was detected in the hydrophobic organic matter (HOM) fraction, and after the COP, and 88.69% of the colority in the HOM was eliminated. Meanwhile, only 59.18% of the colority in the hydrophilic organic matter (HIM) fraction was removed. GC-MS analysis showed that 38 organic pollutant species were completely removed, 8 were partially removed, and 7 were generated. After 90 min of COP treatment, the pharmaceutical EfOM toxicity was effectively reduced based on the higher incubation and lower mortality rates.

With the rapid growth of pharmaceutical needs, large quantities of wastewater containing products, raw materials, solvents and detergents from complex manufacturing processes are generated[1]. Even conventional biological wastewater treatment facilities produce effluent organic matter (EfOM) with high chemical oxygen demand (COD), salinity, color, limited biodegradation, and toxicity[2,3], which increase the potential risk to receiving waters and human health[4]. Therefore, further EfOM removal during pharmaceutical wastewater treatment is an urgent need.

Advanced chemical oxidation processes (AOPs) have attracted much attention for the advanced treatment of industrial wastewater, such as the base process of O_3, H_2O_2, Peroxone, sulfate radical and photocatalytic[5–9]. Among these AOPs, the catalytic ozonation process (COP) has a strong ability to degrade refractory organic pollutants and effectively decolor water via hydroxyl radicals (·OH)[10,11] and broad application potential for wastewater treatment. However, studies on the application of the COP for the advanced treatment of pharmaceutical industrial wastewater have been rarely reported.

For COPs, MnO_x-based catalysts are promising catalysts with great advantages, such as high stability, low water solubility, environmental friendliness and ease of manufacture, and they have been widely studied and applied[12–14]. In addition, porous materials with large surface areas and abundant porous structures have been widely used as metal oxide carriers because of their good performance for increasing the active surface area and adsorption capacity[15,16]. Among these carriers, attapulgite (ATP) is a type of natural, hydrated magnesium silicate mineral with unique pore channels, a large surface area, a high adsorption capacity, and water-insolubility[17–19].

State Key Laboratory of Pollution Control and Resource Reuse, School of the Environment, Nanjing University, N.O.163, Xianlin Avenue, Qixia District, Nanjing, 210023, Jiangsu, PR China. Correspondence and requests for materials should be addressed to K.X. (email: kexu@nju.edu.cn)

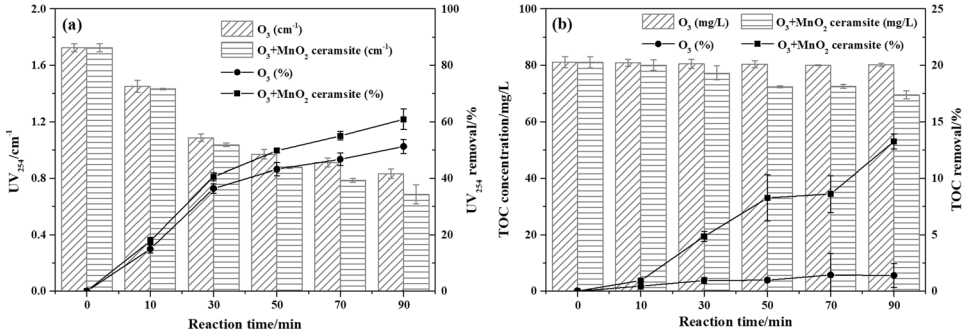

Figure 1. The concentrations and removal efficiencies of UV_{254} (**a**) and TOC (**b**) in the SOP and COP (experimental conditions: pH_0, 3.11; catalyst dosage, 4.0 g/L; gas flow, 400 mL/min; inlet ozone concentration, 20.25 mg/L; reaction volume, 1.0 L; reaction time, 90 min).

Many studies have been performed with the COP to examine removal efficiencies in simulated organic pollution and actual wastewater[12–14]. Lei Zhao *et al.*[12] prepared ceramic, honeycomb-supported manganese catalysts via an impregnation method in a solution of manganese salt and explored the effects of the main operating variables, such as the initial pH, reaction temperature and amount of catalyst, on the degradation efficiency of nitrobenzene. Although the ozonation/Mn-ceramic honeycomb system resulted in a removal rate of approximately 74% for nitrobenzene under the optimal experimental conditions, the quality of the background water was different from that of actual industrial wastewater. Chunmao Chen *et al.*[13] treated heavy oil-refinery wastewater by an integrated ozone and activated carbon-supported manganese oxide method and observed a total organic carbon (TOC) reduction efficiency of 38% due to the catalytic effect. Fengxia Deng *et al.*[14] increased the COD removal efficiency of refinery wastewater by approximately 30% using ozone and alumina-supported manganese and copper oxide catalysts compared with a single ozonation process. In summary, most studies have focused on the following characteristics: (1) new catalyst preparation and characterization of the structure and components, (2) organic pollutant degradation efficiency, (3) the influence of key operating parameters, (4) catalytic mechanism, and (5) catalyst reusability and stability. Thus far, systematic and detailed research on the changes in pharmaceutical EfOM during the COP is lacking.

In this study, ATP was used as a carrier and directly mixed with MnO_2 particles to prepare the MnO_2 ceramsite catalyst. The main aim of this study was to investigate the characteristics, removal, and toxicity of EfOM from a pharmaceutical wastewater treatment plant during a COP in the presence of MnO_2 ceramsite to provide a theoretical basis for advanced treatments of pharmaceutical wastewater using catalytic ozonation technology. The effectiveness of the COP was measured by the UV_{254} and the TOC removal rate of the pharmaceutical wastewater. Second, the color degradation during the COP was explored via Fourier transform infrared (FT-IR) spectroscopy analysis, and the color degradation in the hydrophobicity/hydrophilicity of the EfOM. Then, the changes in the EfOM during the COP were observed by studying the changes in the soluble microbial products (SMPs, containing proteins, polysaccharides, and humic acid), molecular-weight distribution and hydrophobicity/hydrophilicity of the EfOM and performing gas chromatography-mass spectrometer (GC-MS) analyses. Finally, the toxicity of the pharmaceutical EfOM after the COP treatment was assessed to determine its potential risks, as mentioned earlier.

Results and Discussion

UV_{254} and TOC removal. UV_{254} represents the aromatic structure and organic pollutant double bond content[20], and the organic pollutant content in pharmaceutical wastewater can be directly determined via the TOC value. The UV_{254} and TOC removal efficiencies in both the sole ozonation process (SOP) and COP are shown in Fig. 1. The results indicate that the SOP is almost ineffective for TOC removal, but it is quite effective in the destruction of aromatic compounds and double-bond systems. Under the experimental conditions, the UV_{254} and TOC removal efficiencies by the COP were 60.83% and 13.24%, respectively, which were 9.64% and 11.87% higher than those of the SOP. Thus, compared to the SOP, the COP can more completely break aromatic structures and double bonds, and some organic pollutants are mineralized during the COP. Furthermore, there is a strong correlation between the reduction of UV_{254} and the production of ·OH during ozonation[21], which indicates that more ·OH is generated during the COP.

The degradation of UV_{254} during COP can be divided into two parts: the first one is a fast reaction period (0~30 min) with UV_{254} removal efficiency of 40.50%, and the second one is a slow reaction period (30~90 min) with UV_{254} removal efficiency of 20.33%. Previous studies[12,22] have shown that MnO_x-based catalysts can promote the initiation of hydroxyl radicals. Hence, during the COP, a decrease in the UV_{254} value is due to the ozone in the solution and the generation of hydroxyl radicals, which can destroy aromatic structures and double bonds and degrade macromolecular organic compounds into small organic molecules. Ozone can easily react with aromatic compounds with electron-donating groups, but it does not easily react with aromatic compounds with electron-withdrawing groups[23]. During the fast reaction period, the UV_{254} value attributed to aromatic compounds with electron-donating groups quickly decreases due to the dissolved ozone in solution. At the same time, ozone molecules accumulate in the wastewater and are converted to hydroxyl radicals which could react with both electron-donating groups and electron-withdrawing groups. During the slow reaction period, the hydroxyl radicals

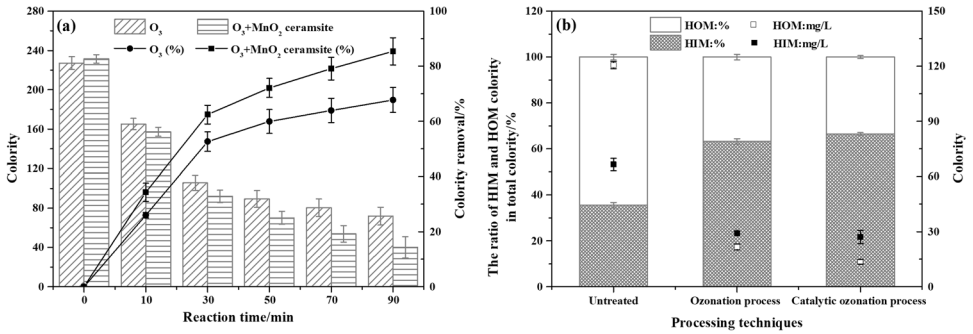

Figure 2. The colority concentration and removal efficiency in the SOP and COP (**a**) and the colority distribution in the untreated HIM and HOM fractions and the HIM and HOM fractions treated with the SOP and COP (**b**) (experimental conditions: pH_0, 3.11; catalyst dosage, 4.0 g/L; gas flow, 400 mL/min; inlet ozone concentration, 20.25 mg/L; reaction volume, 1.0 L; reaction time, 90 min).

can react with aromatic compounds containing electron-withdrawing groups, resulting in a continuous decrease in the UV_{254} value. However, due that the production of hydroxyl radicals in SOP is smaller than COP, COP has a higher UV_{254} removal rate during the slow reaction period, and most fatty compounds with carbonyl and carboxylic acid groups which reacted with ozone would remain their structures till the end of treatment in SOP.

Ozone oxidation of organic matter is selective; i.e., ozone can more easily cleave benzene rings and double bonds to form small organic molecules rather than further degrade the small organic compounds to achieve complete mineralization[24–26]. Therefore, after an ozone treatment for 90 min, the TOC value of the pharmaceutical wastewater remained almost the same, and the TOC removal rate was approximately 1.37%, while the UV_{254} removal efficiency could reach 51.19%. However, upon the addition of MnO_2 ceramsite, a higher concentration of ·OH (the study of ·OH generation could be seen in supporting information), which has no oxidation selectivity, was generated and improved the mineralization rate of the organic matter, resulting in a 13.24% removal rate. The slightly low value of TOC removal rate may be due to the presence of various inorganic anions in wastewater. Inorganic anions, such as chloride ions (Cl^-), sulfate ions (SO_4^{2-}), bicarbonate ions (HCO_3^-) and phosphate ions (PO_4^{3-}), may have an effect on the degradation of organic matter in the COP[27–29]. There are three major anions in the bio-treated pharmaceutical wastewater (BTPW): Cl^-, PO_4^{3-} and NO_3^-. PO_4^{3-}, which is a stronger Lewis base than the water, can substitute for surface OH groups on the catalysts by adsorption on the metal oxide in water[30,31], and is considered hydroxyl radical scavenger[32]. Cl^-, which acts as a typical hydroxyl radical scavenger in aqueous solutions, can react with ozone and ·OH to generate less reactive chlorine species[29,33]. Nevertheless, Zhang *et al.*[34] and Yuan *et al.*[27] found that the introduction of Cl^- could promote the degradation of organics, which was caused by the complex formation between Cl^- and the catalyst and the presence of main oxidizing free radical was O_2^- instead of ·OH. NO_3^- has no significant effect on the removal of organic matter[29].

Decolorization performance. Although the pharmaceutical wastewater was previously treated by hydrolysis acidification, anaerobic-anoxic-oxic (A/A/O) and a moving-bed biofilm reactor (MBBR) in sequence, the water still had a very high colority of 224. An XAD-8 resin was used to separate the BTPW into hydrophilic (HIM) and hydrophobic (HOM) organic matters. Figure 2 shows the concentration and removal efficiency of the colority as well as the distribution of the colority in the HIM and HOM fractions during the SOP and COP. As shown in Fig. 2(b), most of the wastewater colority is concentrated in the HOM fraction, accounting for 64.44% of the total colority. Qi *et al.* stated that in wastewater treatment plant, the hydrophobic fraction contains more unsaturated structures, whereas the hydrophilic fraction contains more carbohydrates or O-alky groups[35]. Figure 2(a) indicates that both the SOP and COP were good at removing the colority. Similar to the degradation of UV_{254}, the colority reaction process can also be divided into a fast reaction period (0~30 min) and a slow reaction period (30~90 min). After 90 min of the COP treatment, 85.42% of the colority was removed, which was 17.66% higher than the removal in the SOP. Additionally, colority of 107.02 was decreased by the COP in the HOM fraction, and the degradation rate was 88.69%, which was 6.67% higher than that of the SOP. However, only 39.39 of the colority was removed by the COP in the hydrophilic wastewater, i.e., a 59.18% degradation rate, which was still 2.98% higher than that of the SOP.

The chromophoric and auxochromic functional groups of organic matter in BTPW could be analyzed by FT-IR spectroscopy (Fig. 3) in the range between 500 and 4000 cm^{-1}. In BTPW, the band at 3348 cm^{-1} could be attributed to $-NH_2$ or -OH[35,36], which are important auxochromic groups, and this band remained after 90 min of the COP treatment. Furthermore, -OH is derived from the carboxyl, phenol and alcohol groups in the samples, and the presence of -OH and $-NH_2$ contributes to the formation of colority. The peak at 2928 cm^{-1} and a low intense peak at 1440 cm^{-1} reflected C-H stretching of the cyclic ring[37,38]. These two peaks disappearing after COP possibly reflected pollutants containing cyclic ring, like 1,4-Dioxane and 1-Cyclohexene-1-carboxylic acid,4-(1,5-dimethyl-3-oxohexyl)-, methyl ester-, [R-(R*,R*)], had been degraded. The peak at 2561 cm^{-1} possibly reflect the asymmetric stretching vibration of –C=C-C=C- in the olefin structure. A peak at 1925 cm^{-1} due to out-of-plane vibration of =C-H in benzene ring[39]. The peak disappeared after the COP, which indicated that the structure of benzene ring was destroyed. The FT-IR spectra showed absorption peaks at 1698, 1664 and 1624 cm^{-1}, which may be due to the stretching vibration of C=C and N=O[40]. After the COP, the peaks at 1698,

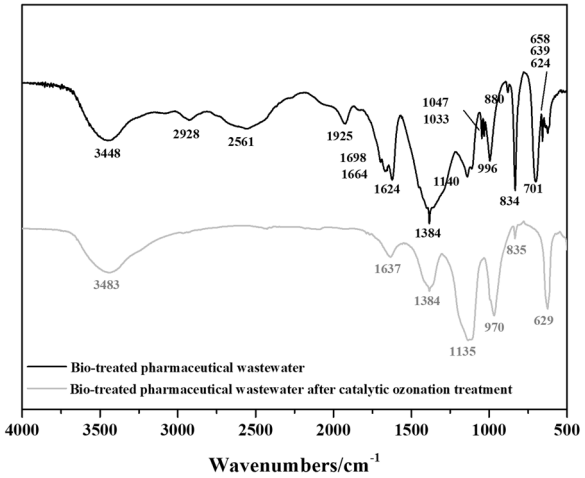

Figure 3. FT-IR spectra of dried samples derived from the BTPW before and after the COP.

1664 and 1624 cm^{-1} significantly weakened to a single peak at 1637 cm^{-1}, which resulted in a decrease in the colority and indicated of formed of C=O in primary amide groups[41,42]. The peak at 1384 cm^{-1} decreased after the COP, which indicated that a bond in -CH_3 was broken. The peaks at 1047 cm^{-1}, 1033 cm^{-1} and 996 cm^{-1} were probably caused by a high concentration of functional groups rich in oxygen with aliphatic structures[43] or -C-O in alcohols and minerals[44], and these bands disappeared after COP. The intense absorption peaks 880 cm^{-1} and 834 cm^{-1} might be due to the out-of-plane O-H bending of aromatics[45]. After COP, the weakening peak at 834 cm^{-1} and disappearance peak at 880 cm^{-1} might be due to the destruction of the aromatics. The bands at 624, 639, 658 and 701 cm^{-1} might be caused by the presence of carboxylate dimers, amines, and amides[46]. After COP, the bands formed at 1135 cm^{-1}, 970 cm^{-1} and 629 cm^{-1}, which might be due to the -C-O stretching vibration in the O-alky group or carbohydrate C-C[35], the C-O-C vibration in ketals or hemiketals and the CNO vibrations in aliphatic nitro compounds[39].

Characteristics of EfOM during the COP. In general, EfOM mainly contains natural organic matter (NOM), SMPs, and trace harmful chemicals, more specifically, EfOM includes proteins, polysaccharides, DNA, humic acid and other components[47]. Figure 4(a–c) shows the concentrations and removal efficiencies of humic acid, protein and polysaccharides for different processes. During the COP, the concentration of humic acid decreased from 325.36 mg/L to 82.73 mg/L, and the removal rate was 74.19%. The protein concentration was reduced by 49.11 mg/L, resulting in a removal rate of 29.36%. Similar trends were observed for the SOP: the removal rate of humic acid and protein was 60.02% and 16.22%, respectively. However, compared with those in the SOP, the removals of humic acid and protein increased by 12.17% and 13.14%, respectively, in the COP. In both the SOP and COP, the polysaccharide content significantly increased when the reaction time was 0~50 min, and the rate of increase in the polysaccharides was far greater in the COP than the SOP. When the reaction time was 50~90 min, the polysaccharide concentration began to decrease in the COP, while in the SOP, the polysaccharide content still increased at a lower rate. After a reaction time of 90 min, the polysaccharide content in the COP was 28.42 mg/L, which was 34.75 mg/L lower than that in the SOP.

Generally, in BTPW, the proteins and polysaccharides mainly consist of macromolecular organic polymers attached to microbial cell walls. Cytoplasm, which contains proteins and polysaccharides, can enter the solution after ozone and hydroxyl radicals directly or indirectly oxidize the cell wall and cell membrane during the COP, leading to an increase in the protein and polysaccharide concentrations. As more hydroxyl radicals are generated, the dissolution of intracellular material is accelerated. However, as the reaction proceeds, the release rate of polysaccharides from cells is less than the ozone and hydroxyl radical degradation rate. Therefore, in the COP, the polysaccharide production rate decreases for reaction times between 0 and 50 min, while the degradation rate increases for reaction times between 50 and 90 min.

The distribution of TOC in the HIM and HOM fractions is shown in Fig. 4(d). The wastewater contained 55.62% of HOM, 37.81 mg/L of TOC, and 44.28% of HIM, and this composition is similar to that observed in reverse osmosis concentrates[48] and municipal wastewater[49]. The hydrophilicity of the EfOM was enhanced by the COP treatment to 74.22%. Similar results were reported by Orta de Velasquez *et al.*[50], Hu *et al.*[51] and Weng *et al.*[48]. The conversion of HOM to HIM is likely a result of organic matter with aromatic rings and alkyl groups, such as humic acid, reacting with O_3 and ·OH to generate hydrophilic reaction products, such as carboxylic acids[52]. In the SOP and COP, the TOC values of HOM increase by 12.94 mg/L and 10.19 mg/L, respectively, while the TOC values of HIM decrease by 18.46 mg/L and 23.80 mg/L, respectively, indicating that more hydrophobic organic matter is converted to hydrophilic organic matter and can be completely mineralized in the COP than the SOP.

Figure 5 reflects the changes in the molecular weights of the HIM and HOM fractions in the BTPW during the different treatment processes (the details of retention time could be seen in supporting information). For the untreated HIM, the weight spectrum contains five peaks, and the 5th peak disappears after the COP, indicating that the hydrophilic small molecule organic substance was degraded. The areas of peaks 1–4 in Fig. 5(a), which have retention times similar to those of peaks 1–4 in Fig. 5(b), significantly increase, which is probably due to the

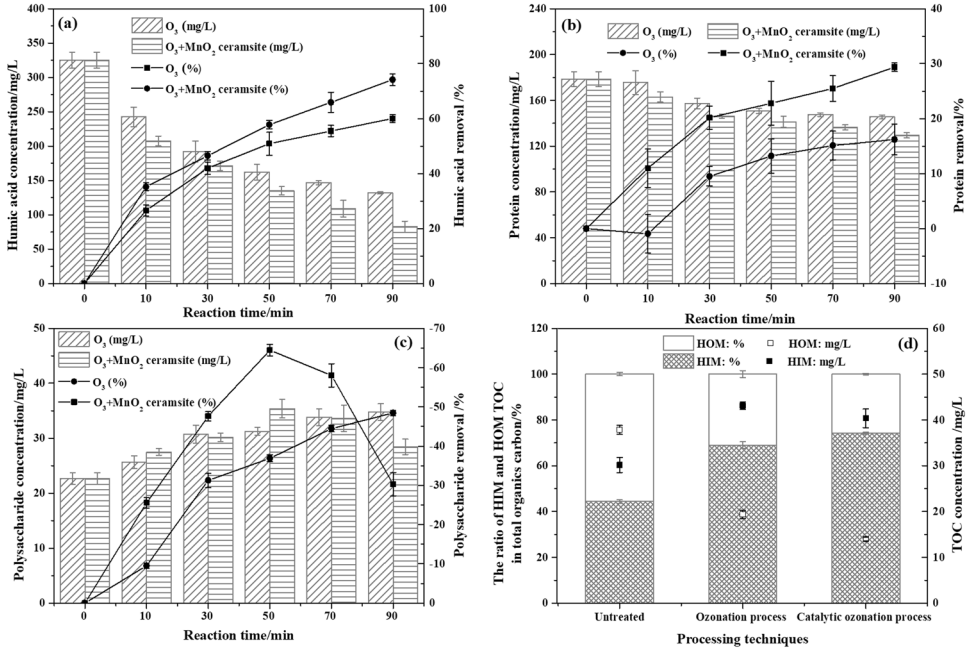

Figure 4. The concentrations and removal efficiencies of humic acid (**a**), protein (**b**) and polysaccharides (**c**) in the SOP and COP, and the distribution of TOC in the untreated HIM and HOM fractions and the HIM and HOM fractions treated with the SOP and COP (**d**) (experimental conditions: pH_0, 3.11; catalyst dosage, 4.0 g/L; gas flow, 400 mL/min; inlet ozone concentration, 20.25 mg/L; reaction volume, 1.0 L; reaction time, 90 min).

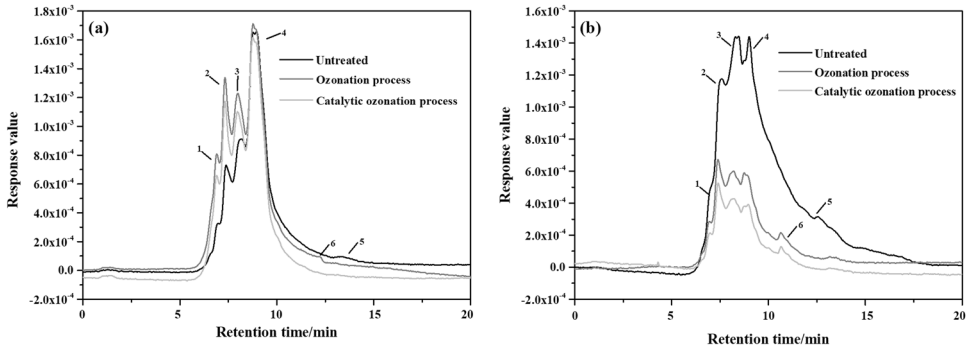

Figure 5. Changes in the molecular weight of untreated HIM and HOM in the BTPW and HIM and HOM fractions treated with the SOP and COP; (**a**) HIM and (**b**) HOM.

conversion of HOM during the COP. The area of peak 4 is almost unchanged in Fig. 5(a), but the area significantly decreases in Fig. 5(b), indicating that the organic matter with a molecular weight of 700–1000 Da is degraded by the COP. For the HOM, the generation of peak 6 after the SOP and COP may result from the oxidation of larger molecular-weight HOM into smaller molecular organic compounds. The molecular-weight distribution of the ozone-treated wastewater is similar to that of the catalytic ozonation-treated samples. In both Fig. 5(a,b), the total peak area for the COP was lower than that for the SOP, indicating that the COP can promote the conversion of more HOM to HIM and increase the degradation rate of HIM.

A total of 45 organic pollutant species were detected by GC-MS in BTPW; after the COP, the content of 8 species decreased, and 38 species were completely removed. Seven new species were generated. The sum of the peak areas for all the organic compounds decreased by 64.27% for the COP, which was 10.37% less than that of the SOP and indicated that organic pollutant species are effectively degraded during the COP. The main organic pollutant species detected with relative peak areas >2% before and after the COP are listed in Table 1. The response value of macromolecular HOM decreased after the COP, which was probably due to the degradation of tetratetracontane, pentacosane, tetracosane and other macromolecule organic matter. In addition, the generation of new acids, esters and ketones, e.g., z-8-methyl-9-tetradecenoic acid, 1,2-benzenedicarboxylic acid, butyl 8-methylnonyl ester and 7,9-di-tert-butyl-1-oxaspiro(4,5)deca-6,9-diene-2,8-dione, enhanced the EfOM hydrophilicity. The reduction in the UV_{254} and colority values was likely a result of the partial degradation of organic compounds with double bonds and benzene rings, such as 2,4-di-tert-butylphenol-,[1,1′-biphenyl]-2,3′-diol,3,4′,5,6′-tetrakis(1,1-dimethylethyl) and 17-pentatriacontene. In summary, the COP can efficiently remove organic pollutants.

Organic compounds	Chemical formula	Raw sample		Catalytic ozonation	
Full name		RPA[a]	PA[b]	RPA	PA
2,4-Di-tert-butylphenol-	$C_{14}H_{22}O$	16.97	1.46E + 06	42.96	1.32E + 06
Tert-butyldimethylsilanol	$C_6H_{16}OSi$	10.57	9.11E + 05	ND[c]	ND
1,4-Dioxane	$C_4H_8O_2$	8.56	7.38E + 05	6.55	2.02E + 05
Diisooctyl phthalate	$C_{24}H_{38}O_4$	5.93	5.11E + 05	8.29	2.55E + 05
Octadecane,3-ethyl-5-(2-ethylbutyl)	$C_{26}H_{54}$	5.35	4.61E + 05	ND	ND
1,2-Benzenedicarboxylic acid, bis(2-methylpropyl) ester	$C_{16}H_{22}O_4$	3.46	2.98E + 05	ND	ND
Tetratetracontane	$C_{44}H_{90}$	3.42	2.95E + 05	ND	ND
Heptacosane	$C_{27}H_{56}$	3.31	2.85E + 05	3.31	1.02E + 05
Benzenamine,N,N-dimethyl-4-[2-(4-quinolinyl)ethenyl]	$C_{19}H_{18}N_2$	3.22	2.77E + 05	ND	ND
Pentacosane	$C_{25}H_{52}$	2.94	2.53E + 05	ND	ND
Tetracosane	$C_{24}H_{50}$	2.56	2.21E + 05	ND	ND
17-Pentatriacontene	$C_{35}H_{70}$	2.54	2.19E + 05	4.15	1.28E + 05
[1,1′-Biphenyl]-2,3′-diol,3,4′,5,6′-tetrakis(1,1-dimethylethyl)	$C_{28}H_{42}O_2$	2.28	1.96E + 05	3.74	1.15E + 05
1,2-Benzenedicarboxylic acid, butyl-8-methylnonyl ester	$C_{22}H_{34}O_4$	ND	ND	9.56	2.95E + 05
Z-8-Methyl-9-tetradecenoic acid	$C_{15}H_{28}O_2$	ND	ND	5.69	1.75E + 05
Octadecane	$C_{18}H_{38}$	ND	ND	3.22	9.91E + 04
7,9-Di-tert-butyl-1-oxaspiro(4,5)deca-6,9-diene-2,8-dione	$C_{17}H_{24}O_3$	ND	ND	2.83	8.71E + 04
Hexadecane	$C_{16}H_{34}$	ND	ND	2.36	7.26E + 04
2-Methylelcosane	$C_{21}H_{44}$	ND	ND	2.29	7.05E + 04
Octadecanal	$C_{18}H_{36}O$	1.19	102903	2.20	6.78E + 04

Table 1. Main organic pollutant species detected by GC-MS before and after the COP. [a]Peak area. [b]Relative peak area (%). [c]ND, not detected.

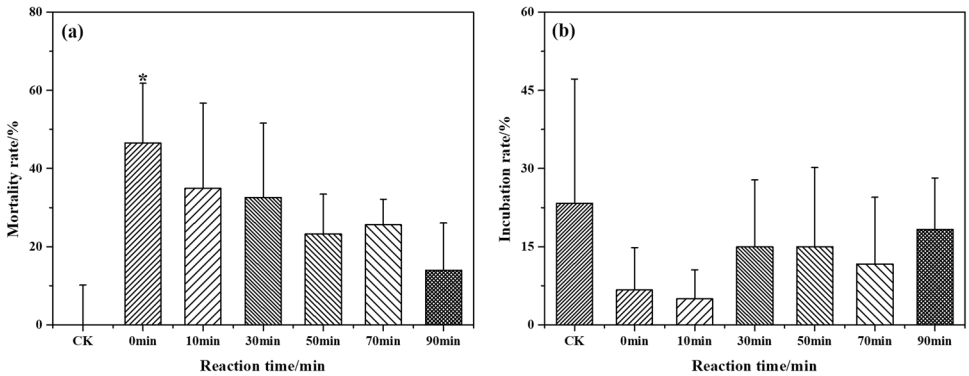

Figure 6. The effect of the COP reaction time on the zebrafish embryo 24 hpf mortality rate (**a**) and 48 hpf incubation rate (**b**).

Toxicity assessment. Although the colority and organic matter were removed from the BTPW by the COP treatment after a reaction time of 90 min, the toxic effects of wastewater on the environment and human health cannot be ignored. A study explored the acute toxicity of reverse osmosis concentrates[48] and showed that ozonation can increase the toxicity of concentrates for zebrafish and cause a higher mortality rate. The 24 hpf mortality and 48 hpf incubation rate of zebrafish embryos were used as acute toxicity assessment indicators in this study, and the results are shown in Fig. 6. Significant differences ($p < 0.05$) in the 24 hpf mortality of the zebrafish embryos existed between the control group and the untreated BTPW. The BTPW had high biological toxicity with a high mortality rate of 46.51% and a low incubation rate of 6.67%. The mortality rate gradually decreased and the incubation rate increased as the COP reaction time increased. At the end of the reaction, the mortality and incubation rates were 13.95% and 18.33%, respectively, which were not significantly different from the control group and indicated that the COP could effectively reduce the toxicity of BTPW. The results show that the COP can effectively eliminate the BTPW toxicity, and this technique can be used as a reliable method for the detoxification of pharmaceutical wastewater.

Conclusions

Experiments were performed to study the removal rates and toxicity of BTPW during the COP in the presence of MnO_2 ceramsite. The following conclusions were obtained:

(1) The COP has a good performance for the removal of TOC and UV_{254} with 60.83% and 13.24% removal rates, respectively. Furthermore, the COP had a high efficiency for the removal of proteins, polysaccharides and humic acid. In addition, the COP can promote the conversion of HOM to HIM and increase the degradation rate of HIM.
(2) The COP removed 85.42% of the colority by destroying –C=C-C=C-, C=O, N=O, and C=C bonds. Furthermore, most of the colority in the HOM was eliminated with an 88.69% degradation rate, whereas only 59.18% of the colority in HIM was removed.
(3) After 90 min of the COP treatment, the BTPW toxicity was effectively reduced, as evidenced by the high incubation and low mortality rates. The GC-MS analysis showed that 38 types of organic pollutant species were completely removed, 8 were partially removed, and 7 were generated, which decreased the number of organic species from 45 to 15.

Experimental

Materials and reagents. BTPW used in this study was obtained from a pharmaceutical wastewater treatment plant located in Zhejiang Province, China. The treatment process for 2000 m^3/d consists of hydrolysis acidification, A/A/O and a MBBR in sequence. All the collected wastewater was passed through a 0.45-μm filter, adjusted to pH = 3.1 ± 0.1 with hydrochloric acid, and stored at 4 °C before use. The main characteristics of the pretreated wastewater used in this study were as follows: 3.1 ± 0.1 pH_0, 244 ± 3 mg/L of COD, 85 ± 2 mg/L of TOC, 224 ± 7 colority, 2050 ± 18 mg/L of chloride ions, 896 ± 7 mg/L of nitrate ions, 186 ± 4 mg/L of phosphate ions.

All chemical reagents were analytical reagent grade and used as received. Ultrapure water (≥18 MΩcm) purified by a Millipore Milli-Q Water system was used throughout this study. The details about the preparation of the MnO_2 ceramsite as well as the methods and results of the characterizations and re-use performance are shown in the supporting information.

Experimental procedure. To better explain the changes in the pharmaceutical EfOM during the COP, the SOP was also studied. SOP and COP were both carried out in a semi-continuous mode in a 1.2 L plexiglass reactor at room temperature by continuously bubbling a mixture of ozone/oxygen (inlet ozone concentration 20.25 ± 0.75 mg/L) through a microporous titanium plate at a flow rate of 400 mL/min. The reactor is a cylinder with a diameter of 80 mm and a height of 360 mm. Ozone was generated through an ozonizer (WH-H-Y, Wohuan Ozone Mechanical and Electrical Equipment Company, China) using dry oxygen as the feed gas. Before the experimental operation of the COP, 1 L of pretreated wastewater and 4 g of MnO_2 ceramsite were first introduced into the reactor, and then, ozone was continuously fed into the reactor. Samples were withdrawn at 0, 10, 30, 50, 70 and 90 min, and the ozone was immediately quenched by sodium thiosulfate. After the ozone quenching, the samples were filtered by a 0.45-μm Teflon filter (Pall Corporation, USA) for analysis. After each run, the reactor was repeatedly washed with 20% hydrochloride acid and Milli-Q water. The device diagram for the experimental reaction is shown in Fig. S1. The SOP was carried out in an ozonation reactor under the same conditions without MnO_2 ceramsite. Each process was performed in triplicate.

The toxicity assignment experimental steps were as follows. The organic matter was extracted from the water samples by Oasis HLB SPE cartridges, sequentially eluted with methanol and 1:1 n-hexane/acetone and then dissolved in DMSO after nitrogen blowing. The organic matter was diluted before use. Wild-type zebrafish were obtained from the Model Animal Research Center of Nanjing University. Embryos were obtained from 2 males and 1 female in a tank stimulated by the onset of light. The embryos were collected and placed at 28.5 °C in Petri dishes. Hours post fertilization (hpf) was used to represent the age of the embryos. Embryos at 4 hpf were randomly distributed in a 24-well plate at a density of 15 embryos/well at 28.5 °C with 2 mL of the diluted water samples. Dead embryos were removed daily to prevent necrotic effects. Each treatment was performed in quadruplicate.

Analytical method. The ozone concentration in the gas phase was obtained by adopting an iodometric method[53]. The TOC and UV_{254} were analyzed by an Aurora 1030 W TOC analyzer (OI Analytical, USA) and a 2540 UV spectrophotometer (Shimadzu, Japan), respectively. The colority was measured by a colorimetic method according to the Chinese SEPA standard method[54]. The concentrations of humic acid, polysaccharides, and proteins were quantified by an improved Lowry method[55], a colorimetric method[56], and a bicinchoninic acid (BCA) kit method, respectively. Inorganic anions were determined by ion chromatography in a Dionex ICS-1000 apparatus equipped with an IonPac AS22 4 × 250 mm analytical column. The mobile phase was 4.5 mM Na_2CO_3 and 1.4 mM $NaHCO_3$ with a flow rate of 1.2 mL/min at 30 °C. An XAD-8 macroporous adsorption resin was used to separate the hydrophilic and hydrophobic organic compounds in the water samples, according to Liu's method[57]. The water samples were freeze-dried by a lyophilizer (Lacbconco, USA), and analyzed by a NEXUS 870 Fourier transform infrared spectrometer (NICOLET, USA). The distribution of the molecular weight was analyzed by high performance liquid chromatography-size exclusion chromatography (HPSEC) with a gel permeation column (Protein Pak 125, 7.8 × 300 mm, 10 μm, Waters)[58]. The compound identification was peformed by a 7890 A gas chromatograph (Agilent, USA) interfaced with a 5977B mass selective detector (Agilent, USA). The details of distribution of the molecular weight and GC-MS analysis procedure could be seen in supporting information. A mortality rate of 24 hpf and an incubation rate of 48 hpf were assessed using an SMZ745T dissecting microscope (Nikon, Japan).

Statistical analysis. A statistical difference was evaluated using one-way analysis of variance (ANOVA). All analyses were performed by an SPSS statistical package (SPSS Inc., U.S.A.). A P value < 0.05 was accepted as significance and is marked with "*".

Data availability statement. The data within my uploaded manuscript file is available.

References

1. Martínez, F. *et al*. Techno-economical assessment of coupling Fenton/biological processes for the treatment of a pharmaceutical wastewater. *J. Environ. Chem. Eng.* **6**, 485–494 (2017).
2. Ng, K. K., Shi, X. Q., Ong, S. L., Lin, C. F. & Ng, H. Y. An innovative of aerobic bio-entrapped salt marsh sediment membrane reactor for the treatment of high-saline pharmaceutical wastewater. *Chem. Eng. J.* **295**, 317–325 (2016).
3. Kaya, Y. *et al*. Treatment of chemical synthesis-based pharmaceutical wastewater in an ozonation-anaerobic membrane bioreactor (AnMBR) system. *Chem. Eng. J.* **322**, 293–301 (2017).
4. Hernando, M. D., Mezcua, M., Fernandez-Alba, A. R. & Barcelo, D. Environmental risk assessment of pharmaceutical residues in wastewater effluents, surface waters and sediments. *Talanta* **69**, 334–342 (2006).
5. Boczkaj, G. & Fernandes, A. Wastewater treatment by means of advanced oxidation processes at basic pH conditions: A review. *Chem. Eng. J.* **320**, 608–633 (2017).
6. Gągol, M., Przyjazny, A. & Boczkaj, G. Wastewater treatment by means of advanced oxidation processes based on cavitation – A review. *Chem. Eng. J.* **338**, 599–627 (2018).
7. Boczkaj, G., Gągol, M., Klein, M. & Przyjazny, A. Effective method of treatment of effluents from production of bitumens under basic pH conditions using hydrodynamic cavitation aided by external oxidants. *Ultrasonics Sonochemistry* **40**, 969–979 (2018).
8. Boczkaj, G., Fernandes, A. & Makoś, P. Study of different advanced oxidation processes for wastewater treatment from petroleum bitumen production at basic pH. *Industrial & Engineering Chemistry Research* **56**, 8806–8814 (2017).
9. Gągol, M., Przyjazny, A. & Boczkaj, G. Highly effective degradation of selected groups of organic compounds by cavitation based AOPs under basic pH conditions. *Ultrasonics Sonochemistry* **45**, 257–266 (2018).
10. Ghatak, H. R. Advanced oxidation processes for the treatment of biorecalcitrant organics in wastewater. *Crit. Rev. Env. Sci. Tec.* **44**, 1167–1219 (2014).
11. Nawrocki, J. & Kasprzyk-Hordern, B. The efficiency and mechanisms of catalytic ozonation. *Appl. Catal. B-Environ.* **99**, 27–42 (2010).
12. Zhao, L., Ma, J., Sun, Z. Z. & Zhai, X. D. Catalytic ozonation for the degradation of nitrobenzene in aqueous solution by ceramic honeycomb-supported manganese. *Appl. Catal. B-Environ.* **83**, 256–264 (2008).
13. Chen, C. M., Wei, L. Y., Guo, X., Guo, S. H. & Yan, G. X. Investigation of heavy oil refinery wastewater treatment by integrated ozone and activated carbon -supported manganese oxides. *Fuel Process. Technol.* **124**, 165–173 (2014).
14. Deng, F. X., Qiu, S., Chen, C., Ding, X. & Ma, F. Enhanced CO oxidation rates at the interface of mesoporous oxides and Pt nanoparticles. *Ozone-Sci. Eng.* **37**, 546–555 (2015).
15. Xing, S. T. *et al*. Catalytic ozonation of sulfosalicylic acid over manganese oxide supported on mesoporous ceria. *Chemosphere* **144**, 7–12 (2016).
16. Sun, Q. Q. *et al*. Influence of the surface hydroxyl groups of MnOx/SBA-15 on heterogeneous catalytic ozonation of oxalic acid. *Chem. Eng. J.* **242**, 348–356 (2014).
17. Li, B., Li, L. W., Zhang, Q., Weng, W. Z. & Wan, H. L. Attapulgite as natural catalyst for glucose isomerization to fructose in water. *Catal. Commun.* **99**, 20–24 (2017).
18. Zhang, T. & Nan, Z. R. Decolorization of Methylene Blue and Congo Red by attapulgite-based heterogeneous Fenton catalyst. *Desalin. Water Treat.* **57**, 1–8 (2014).
19. Li, X. Y., Zhang, D. Y., Liu, X. Q., Shi, L. Y. & Sun, L. B. A tandem demetalization-desilication strategy to enhance the porosity of attapulgite for adsorption and catalysis. *Chem. Eng. Sci.* **141**, 184–194 (2016).
20. Zhang, T., Lu, J. F., Ma, J. & Qiang, Z. M. Comparative study of ozonation and synthetic goethite-catalyzed ozonation of individual NOM fractions isolated and fractionated from a filtered river water. *Water Res.* **42**, 1563–1570 (2008).
21. Audenaert, W. T., Vandierendonck, D., Van Hulle, S. W. & Nopens, I. Comparison of ozone and HO· induced conversion of effluent organic matter (EfOM) using ozonation and UV/H_2O_2 treatment. *Water Res.* **47**, 2387–2398 (2013).
22. Xing, S. T., Hu, C., Qu, J. H., He, H. & Yang, M. Characterization and reactivity of MnOx supported on mesoporous zirconia for herbicide 2,4-D mineralization with ozone. *Environ. Sci. Technol.* **42**, 3363–3368 (2008).
23. Wang, Q. *et al*. Heterogeneous catalytic ozonation of natural organic matter with goethite, cerium oxide and magnesium oxide. *RSC Adv* **6**, 14730–14740 (2016).
24. Shahidi, D., Roy, R. & Azzouz, A. Advances in catalytic oxidation of organic pollutants - Prospects for thorough mineralization by natural clay catalysts. *Appl. Catal. B-Environ.* **174**, 277–292 (2015).
25. Hoigné, J. & Bader, H. Rate constants of reactions of ozone with organic and inorganic compounds in water—II: dissociating organic compounds. *Water Res.* **17**, 185–194 (1983).
26. Gong, J. L., Liu, Y. D. & Sun, X. B. O_3 and UV/O_3 oxidation of organic constituents of biotreated municipal wastewater. *Water Res.* **42**, 1238–1244 (2008).
27. Yuan, X. J. *et al*. Enhanced ozonation degradation of atrazine in the presence of nano-ZnO: performance, kinetics and effects. *J. Environ. Sci-China* **61**, 3–13 (2017).
28. Petre, A. L., Carbajo, J. B., Rosal, R., Garcia-Calvo, E. & Perdigon-Melon, J. A. CuO/SBA-15 catalyst for the catalytic ozonation of mesoxalic and oxalic acids. Water matrix effects. *Chem. Eng. J.* **225**, 164–173 (2013).
29. Wu, K., Zhang, F., Wu, H. & Wei, C. The mineralization of oxalic acid and bio-treated coking wastewater by catalytic ozonation using nickel oxide. *Environ. Sci. Pollut. Res*., 1–12, (2017).
30. Zhang, T. & Ma, J. Catalytic ozonation of trace nitrobenzene in water with synthetic goethite. *Journal of Molecular Catalysis A: Chemical* **279**, 82–89 (2008).
31. Afzal, S., Quan, X., Chen, S., Wang, J. & Muhammad, D. Synthesis of manganese incorporated hierarchical mesoporous silica nanosphere with fibrous morphology by facile one-pot approach for efficient catalytic ozonation. *J. Hazard. Mater.* **318**, 308–318 (2016).
32. Kasprzyk-Hordern, B., Ziolek, M. & Nawrocki, J. Catalytic ozonation and methods of enhancing molecular ozone reactions in water treatment. *Appl. Catal. B-Environ.* **46**, 639–669 (2003).
33. Wang, Z. H., Yuan, R. X., Guo, Y. G., Xu, L. & Liu, J. S. Effects of chloride ions on bleaching of azo dyes by Co^{2+}/oxone regent: Kinetic analysis. *J. Hazard. Mater.* **190**, 1083–1087 (2011).
34. Zhang, J., Wu, Y., Liu, L. & Lan, Y. Rapid removal of p-chloronitrobenzene from aqueous solution by a combination of ozone with zero-valent zinc. *Sep. Purif. Technol.* **151**, 318–323 (2015).
35. Qi, W. X., Zhang, H., Hu, C. Z., Liu, H. J. & Qu, J. H. Effect of ozonation on the characteristics of effluent organic matter fractions and subsequent associations with disinfection by-products formation. *Sci. Total Environ.* **610**, 1057–1064 (2018).
36. Liakos, T. I. & Lazaridis, N. K. Melanoidins removal from simulated and real wastewaters by coagulation and electro-flotation. *Chem. Eng. J.* **242**, 269–277 (2014).

37. Selvi, A., Salam, J. A. & Das, N. Biodegradation of cefdinir by a novel yeast strain, Ustilago sp. SMNO$_3$ isolated from pharmaceutical wastewater. *World Journal of Microbiology and Biotechnology* **30**, 2839–2850 (2014).
38. Babu, B. R., Venkatesan, P., Kanimozhi, R. & Basha, C. A. Removal of pharmaceuticals from wastewater by electrochemical oxidation using cylindrical flow reactor and optimization of treatment conditions. *Journal of Environmental Science and Health, Part A* **44**, 985–994 (2009).
39. Jinxi, X. *Infrared spectroscopy: applications in organic chemistry and medicinal chemistry*. (Science Press, 1987).
40. Ma, H. Z., Zhuo, Q. F. & Wang, B. Electro-catalytic degradation of methylene blue wastewater assisted by Fe_2O_3-modified kaolin. *Chem. Eng. J.* **155**, 248–253 (2009).
41. Gracia, R., AragÜEs, J. L. & Ovelleiro, J. L. Mn (II)-catalysed ozonation of raw Ebro river water and its ozonation by-products. *Water Res.* **32**, 57–62 (1998).
42. Zhuang, H. F. *et al*. Advanced treatment of biologically pretreated coal gasification wastewater by a novel heterogeneous Fenton oxidation process. *J. Environ. Sci-China* **33**, 12–20 (2015).
43. Zhu, L. *et al*. Component analysis of extracellular polymeric substances (EPS) during aerobic sludge granulation using FTIR and 3D-EEM technologies. *Bioresource Technol.* **124**, 455–459 (2012).
44. Zhang, M., Wang, Z., Li, P. H., Zhang, H. & Xie, L. Bio-refractory dissolved organic matter and colorants in cassava distillery wastewater: characterization, coagulation treatment and mechanisms. *Chemosphere* **178**, 259–267 (2017).
45. Yao, Z. Y., Qi, J. H. & Wang, L. H. Isolation, fractionation and characterization of melanin-like pigments from chestnut (Castanea mollissima) shells. *J. Food Sci.* **77**, C671–C676 (2012).
46. Hatano, K. I., Kikuchi, S., Miyakawa, T., Tanokura, M. & Kubota, K. Separation and characterization of the colored material from sugarcane molasses. *Chemosphere* **71**, 1730–1737 (2008).
47. Shon, H. K., Vigneswaran, S. & Snyder, S. A. Effluent organic matter (EfOM) in wastewater: constituents, effects, and treatment. *Crit. Rev. Env. Sci. Tec.* **36**, 327–374 (2006).
48. Weng, J., Jia, H., Wu, B. & Pan, B. Is ozonation environmentally benign for reverse osmosis concentrate treatment? Four-level analysis on toxicity reduction based on organic matter fractionation. *Chemosphere* **191**, 971–978 (2018).
49. Zheng, X., Khan, M. T. & Croue, J. P. Contribution of effluent organic matter (EfOM) to ultrafiltration (UF) membrane fouling: isolation, characterization, and fouling effect of EfOM fractions. *Water Res.* **65**, 414–424 (2014).
50. de Velasquez, M. T. O., Monje-Ramirez, I. & Paredes, J. F. M. Effect of ozone in UF-membrane flux and dissolved organic matter of secondary effluent. *Ozone-Sci. Eng.* **35**, 208–216 (2013).
51. Hu, J. Y., Ong, S. L., Shan, J. H., Kang, J. B. & Ng, W. J. Treatability of organic fractions derived from secondary effluent by reverse osmosis membrane. *Water Res.* **37**, 4801–4809 (2003).
52. Van Geluwe, S., Braeken, L. & Van der Bruggen, B. Ozone oxidation for the alleviation of membrane fouling by natural organic matter: A review. *Water Res.* **45**, 3551–3570 (2011).
53. Rakness, K. *et al*. Guideline for measurement of ozone concentration in the process gas from an ozone generator. *Ozone-Sci. Eng.* **18**, 209–229 (1996).
54. China, E. O. Water and Wastewater Monitoring Analysis Method(fourth ed.). *Chinese Environment Science Publisher*, (Beijing (2002)).
55. Shen, Y. X., Xiao, K., Liang, P., Ma, Y. W. & Huang, X. Improvement on the modified Lowry method against interference of divalent cations in soluble protein measurement. *Appl. Microbiol. Biotechnol.* **97**, 4167–4178 (2013).
56. Dubois, M., Gilles, K. A., Hamilton, J. K., Rebers, P. A. & Smith, F. Colorimetric method for determination of sugars and related substances. *Anal. Chem.* **28**, 350–356 (1956).
57. Liu, H. Z., Jeong, J., Gray, H., Smith, S. & Sedlak, D. L. Algal uptake of hydrophobic and hydrophilic dissolved organic nitrogen in effluent from biological nutrient removal municipal wastewater treatment systems. *Environ. Sci. Technol.* **46**, 713–721 (2012).
58. Wang, D. *et al*. Chromium speciation in tannery effluent after alkaline precipitation: Isolation and characterization. *J. Hazard. Mater.* **316**, 169–177 (2016).

Acknowledgements

This study was financially supported by the Technology Research and Development Program of Jiangsu Province, China (BE2016735) and National Water Pollution Control and Governance of Science and Technology Major Special (No. 2017ZX07202-001).

Author Contributions

S.H.W. wrote the manuscript and researched data. L.C. and W.Q.L. contributed to the experiments. H.Q.R., H.D.H., B.W., and K.L. reviewed manuscript. K.X. reviewed/edited manuscript. All authors reviewed the paper.

Additional Information

Supplementary information accompanies this paper at https://doi.org/10.1038/s41598-018-27921-0.

Competing Interests: The authors declare no competing interests.

Publisher's note: Springer Nature remains neutral with regard to jurisdictional claims in published maps and institutional affiliations.